Study of Deformation Mechanisms in Titanium by Interrupted Rolling and Channel Die Compression Tests

Lei Bao, Christophe Schuman, J.S. Lecomte, Marie Jeanne Philippe, Xiang Zhao, Liang Zuo, Claude Esling

 CMC, vol.15, no.2, pp.113-127, 2010

Study of Deformation Mechanisms in Titanium by Interrupted Rolling and Channel Die Compression Tests

Lei Bao[1,2], Christophe Schuman[1], Jean-sébastien Lecomte[1] Marie-Jeanne Philippe[1], Xiang Zhao[2], Liang Zuo[2] and Claude Esling[1]

Abstract: The mechanisms of small plastic deformation of titanium (T40) during cold rolling and channel die compression by means of "interrupted in situ" EBSD orientation measurements were studied. These interrupted EBSD orientation measurements allow to determine the rotation flow field which leads to the development of the crystallographic texture during the plastic deformation. Results show that during rolling, tension twins and compression twins occur and various glide systems are activated, the number of grains being larger with twins than with slip traces. In channel die compression, only tension twins are observed in some grains, whereas slip traces can be spotted in almost all observed grains. The different stress conditions and different strain rates existing under the two modes of deformation lead to the activation of different deformation mechanisms.

Keywords: titanium, deformation mechanism, twinning, gliding, orientation, EBSD

1 Introduction

The mechanism of plastic deformation has been studied in some detail in the past [Yoo (1981); McDarmaid, Bowen and Partridge (1984); Vedoya, Pochettino and Penelle (1988); Philippe, Serghat, Houtte, and Esling (1995); Panchanadeeswaran, Doherty and Becker (1996); Kalidindi, Bhattacharyya and Doherty (2004); Prasannavenkatesan, Li, Field and Weiland (2005); Merriman, Field and Trivedi (2008); Skrotzki, Toth, Kloden, Brokmeier and Arruffat-Massion (2008); Quey, Piot and Driver (2010)]. Many efforts have been made in studying deformation twinning and gliding in single and polycrystalline metals [Akhtar (1975); Akhtar, Teghtsoonian and Cryst (1975); Kalidindi (1998); Field, True, Lillo and Flinn (2004); Jiang, Jonas, Mishra, Luo, Sachdev and Godet (2007); Jiang and Jonas (2008)]. The me-

[1] LETAM, CNRS FRE 3143 (former UMR 7078) University of Metz, 57045 Metz, France
[2] Laboratory for Anisotropy and Texture of Materials (MOE), NEU, Shenyang, 110004, China

chanical response of titanium, like other HCP metals, is strongly dependent on the combination of active deformation modes: gliding and twinning. The specific deformation mechanisms depend on the c/a ratio, the available deformation modes, the critical resolved shear stress (CRSS) for gliding, the twin activation stress as well as the imposed deformation relative to the crystallographic texture. According to previous work, $\{10\bar{1}2\}$ tension twins, $\{11\bar{2}1\}$ tension twins and $\{11\bar{2}2\}$ compression twins are activated during plastic deformation at room temperature. Due to the compacity ratio c/a <1.633 in titanium, prismatic glide is the easiest one at room temperature but basal and pyramidal glide were also observed [Pochettino, Gannio, Edwards and Penelle (1992)].

However the previous studies concerning the texture and deformation modes were mostly performed after a certain amount of deformation either by of X-ray diffraction (XRD) or by transmission electron microscopy (TEM). Therefore the initial orientation of the individual grains and the evolution of the orientation flow during deformation were not documented. Moreover, after a certain amount of deformation, twinning and gliding were both active and interacted with each other. Thus it was difficult to resolve the specific orientation condition to activate each deformation mode (either twinning or gliding). Therefore, the present work is devoted to these aspects, providing the lack of information in the literature. In order to follow the evolution of individual orientations during the deformation and to determine the effect of initial orientation on the deformation modes, an interrupted "in situ" EBSD investigation method was proposed. In this method, we follow a sufficient number of grains and perform EBSD measurement in the same area, prior to and after the deformation. Thus it is possible to acquire detailed orientation information of these grains in the interrupted step of deformation and identify the active deformation modes.

2 Experimental

The as-received material was hot-rolled and then annealed commercial purity titanium sheet of 1.5 mm thickness with the composition given in table 1.

Table 1: Chemical composition of commercially pure titanium T40

Elements	H	C	N	O	Fe	Ti
Composition ppm(wt.)	3	52	41	1062	237	Balance

In order to obtain a twin-free microstructure with equiaxed grains, a grain growth annealing was performed at 750°C for 2 hours. After the annealing, the samples were mechanically and then electrolytically-polished in a solution of 200 ml per-

chloric acid in 800 ml methanol at 17V (30 seconds) and at a temperature of 5°C before deformation. Then, the samples were cold rolled or compressed in channel die in two passes respectively, first to 10 % and then to 20% reduction. To perform interrupted "in situ" measurement, a $500\times300\mu m^2$ area was carefully polished and marked out with four micro-indentations. The orientation of all the grains in this polished area was measured by SEM/EBSD before and after each deformation step. The rolling and channel die compression layout is illustrated in Fig. 1. Both sheets of the sandwich were firmly stuck together to avoid any surface sliding during the rolling in order to maintain a good surface quality. EBSD measurements were performed with a JEOL-6500F SEM with a step size of 0.4 μm. The evolution of grain orientation during deformation will be presented later both by pole figures and orientation flow fields.

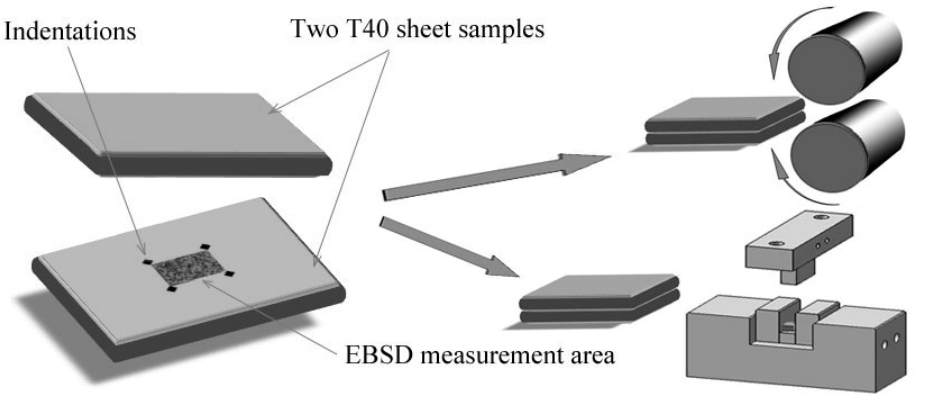

Figure 1: The preparation of samples and arrangement of the rolling and channel die compression tests

3 Deformation in rolling

The orientation map of the grain growth annealed sample shown in Fig. 2 (a) reveals a completely recrystallized microstructure with an average grain size of 10 μm. The {0002}-pole figure (PF) in Fig. 2 (b) shows two strong maxima at $\pm30^\circ$ tilted from ND towards TD, whereas the $\{10\bar{1}0\}$ PF displays the maximum pole densities parallel to RD. In this work, the setting of the coordinate systems and the Euler angles $\{\phi1,\Phi,\phi2\}$ are defined according to Bunge's convention, see Bunge, Esling and Muller (1980).

The lattice rotation was studied after each rolling pass. The orientation of each

individual grain was carefully determined, so that the lattice rotation of each grain could be brought in relation to its own orientation as well as to that of its neighbouring grains. It was found that $\{11\bar{2}2\}$ compression twins (the misorientation between the twin and its matrix corresponds to a 65° rotation about their common <$10\bar{1}0$> axis) and $\{10\bar{1}2\}$ tension twins (85° about <$1\bar{2}10$> axis [Philippe, Esling and Hocheid(1988)]) were most frequently observed (Fig 3). The respective amount of these two types of twinning was further presented by means of the misorientation-angle distributions in Fig. 4. It is seen that after 10% rolling (Fig. 4 (b)), 65° misorientation occurs most frequently, suggesting that $\{11\bar{2}2\}$ twinning was predominant at this stage of deformation. This result is reasonable considering that the initial orientation favors the activation of this compression twin. Whereas when rolling continues to 20%, $\{10\bar{1}2\}$ tension twinning was remarkably increased (Fig. 4 (c)). The orientation analysis could be studied from the microscopic point of view of the crystal reorientation step by step, in terms of the rotation flow field. A small arrow is plotted in the Euler space between the initial grain orientation and the final grain orientation. This field of small arrows offers a graphical representation of the rotational flow field. The flow field can be defined and plotted in the Euler space, and represents an efficient tool to describe the texture evolution through modeling, e.g. Clement and Coulomb (1979), Bunge and Esling (1984), Knezevic, Kalidindi and Fullwood(2008).

In the present case of hexagonal material, due to the particular importance of the c-axes, we choose to plot the small arrows linking the initial orientation and the final orientation in the two dimensional [0001] pole figures. For further discussion, it was of interest to plot separately the rotation flow field of the grains without twins on the one hand (Fig.5 (a)) and the rotation flow field of the matrix of the grains with twins (Fig. 5 (b)). It is seen from Fig 5 that both orientation flow fields are similar, but for a smaller amplitude of the rotation of the matrix of twinned grains, as compared with that of the grains without twins.

Thanks to the interrupted "in situ" method used in the present work, we can follow the evolution of the twins (from nucleation to growth) in each grain. Fig. 6 shows one selected grain before and after each rolling pass. In the figure, the blue lines represent the $\{10\bar{1}2\}$ twin boundaries and the red lines the $\{11\bar{2}2\}$ twin boundaries. It is interesting to find that $\{11\bar{2}2\}$ compression twin appears in the grains with c-axes close to ND. The twinned part grows during the deformation process and the c-axes of the twinned part, reoriented 65° to those of the matrix, are in an orientation favorable for the activation of the $\{10\bar{1}2\}$ tension twin. Subsequently, $\{10\bar{1}2\}$ tension twin activates inside this "new grain" formed by the primary compression twin, and this new secondary twin builds a double twin. So two types of twins, tension and compression twins can form in one and the same grain, compression

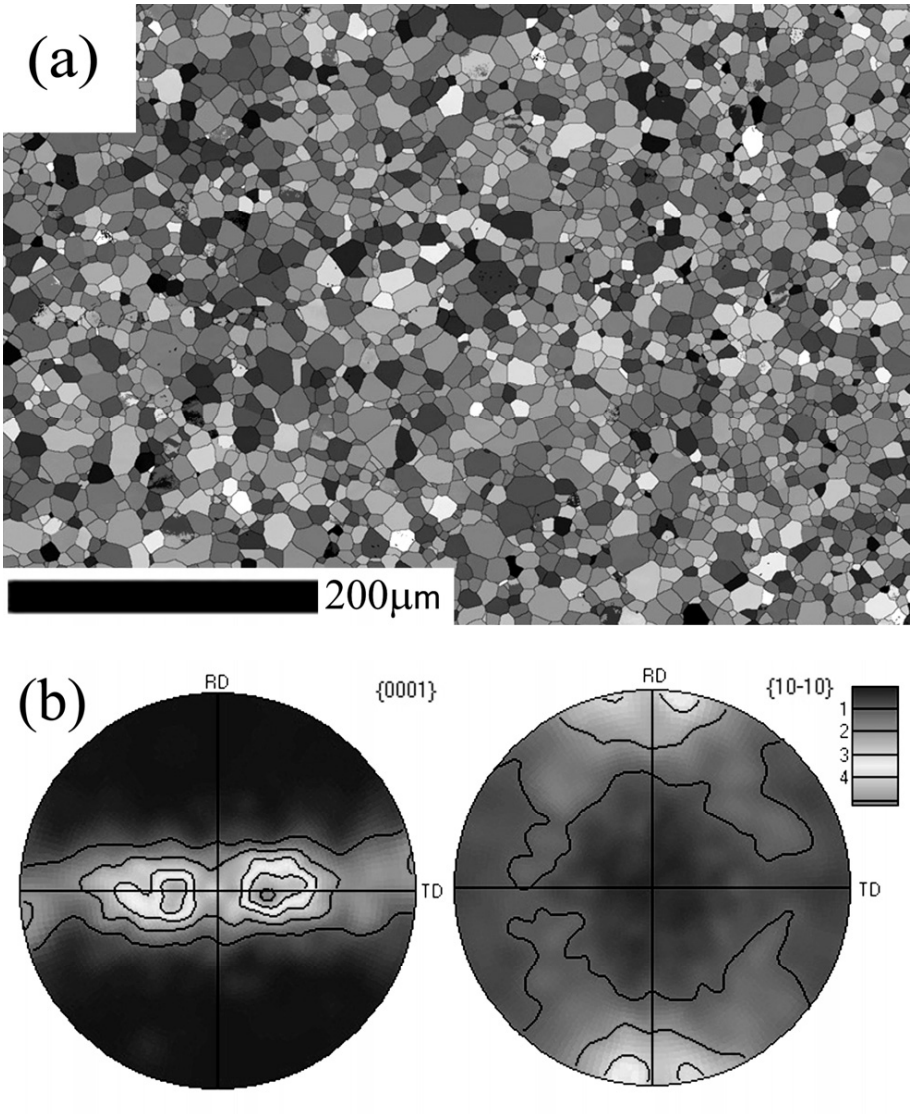

Figure 2: EBSD orientation mapping (a) and 0002, pole figures (b).

twins as first order and tension twins as second order twins. In other words, the $\{11\bar{2}2\}$ twinning brings the c-axis of the twinned part out of the stable orientation. The twinned part is favorably oriented to initiate a tension twin. Then the $\{10\bar{1}2\}$ tension twin forms, reorienting the c-axis of the newly twinned part into a stable orientation.

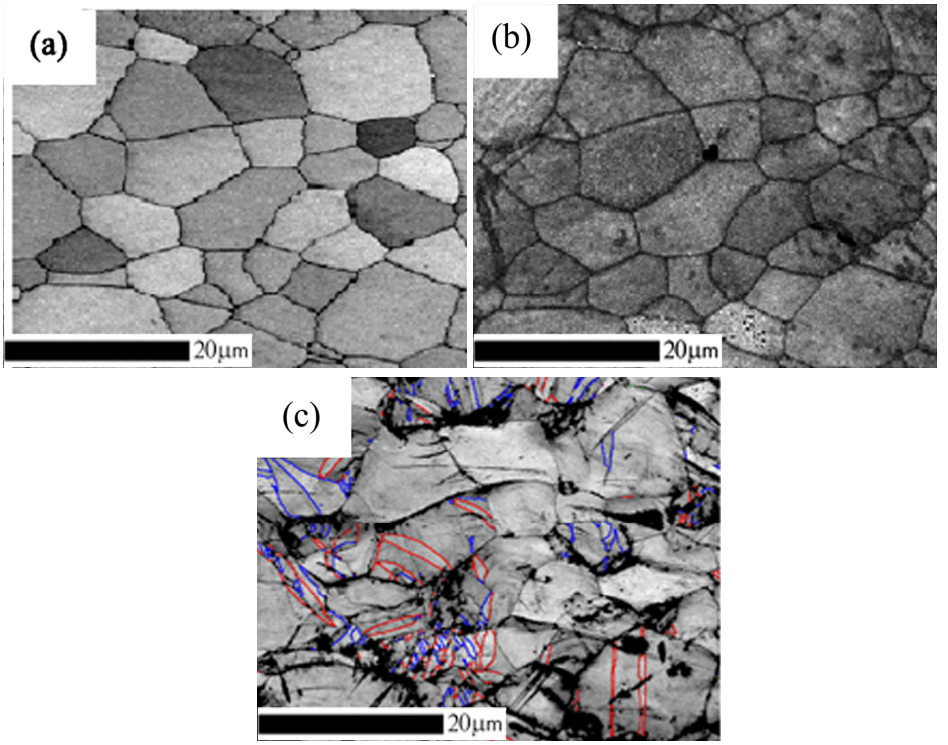

Figure 3: Orientation micrograph of one selected area, before rolling (a), after 10% (b) and 20% (c) rolling. Blue lines: $\{10\bar{1}2\}$ twin boundaries; red lines: $\{11\bar{2}2\}$ twin boundaries.

Slip traces are observed in some grains in the post-deformation EBSD map. In order to identify the activated glide systems corresponding to the traces observed, the possible traces of all possible glide planes [Partridge (1967)] are calculated in the crystal coordinate system, using the orientation data of the related grains and comparing with the observed traces. Consequently, basal <a>, prismatic <a> and pyramidal <a> or <c+a> glide systems are identified in this work.

4 Deformation in channel die compression

In channel die compression, only one type of twin - $\{10\bar{1}2\}$ tension twin is observed and the amount of twinned grains is very low, only 1.07% of the observed grains, which cannot be clearly resolved from the misorientation-angle distribution

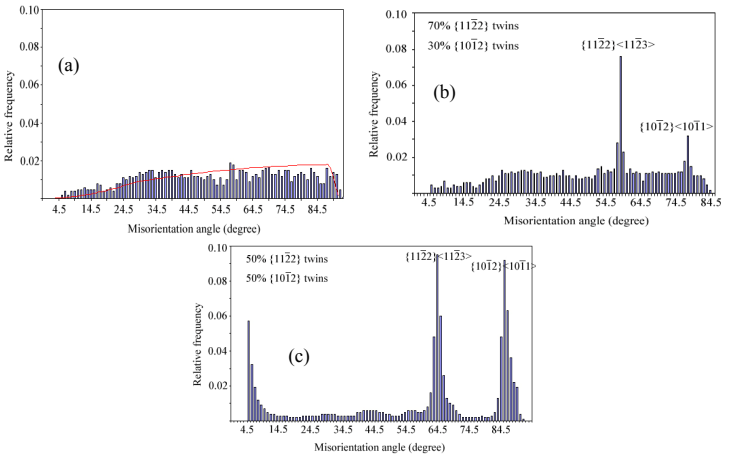

Figure 4: Misorientation-angle distributions of samples deformed to 0% (a), 10% (b) and 20% (c) reduction.

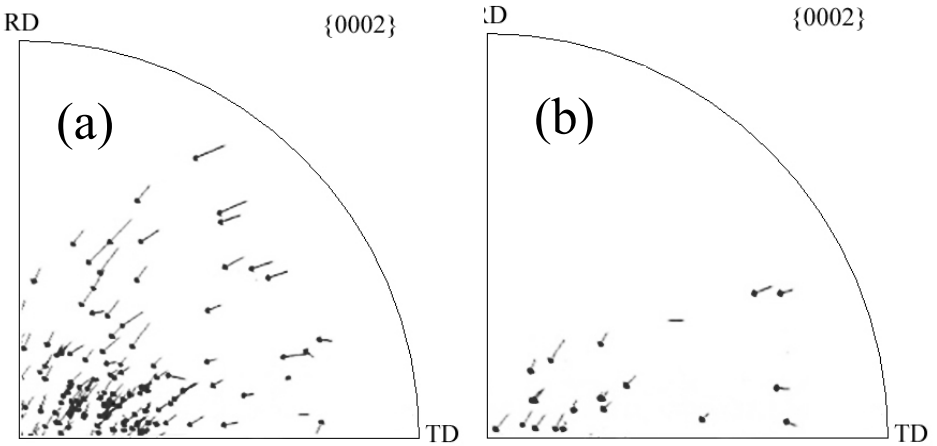

Figure 5: Rotational flow field in grains showing no twins (a). Lattice rotation field in untwinned part (or matrix) of grains showing twins (b).

diagram in Fig. 7.

Compared with rolling, numerous slip traces are observed in a great number of grains in EBSD maps after channel die compression. Using the above trace com-

parison method, basal <a>, prismatic <a> and pyramidal <a> or <c+a> glide are identified. A statistical set of 100 randomly selected grains with slip traces is studied. The occurrence of various glide systems in the studied grains is listed in Table 2. It is seen that among the activated glide systems, 11% are basal <a>, 51% are prismatic <a> and 38% are pyramidal <c+a> or <a>. The Schmid factors for the three glide systems were calculated, and the calculation indicated that most grains have high Schmid factors for pyramidal <c+a> glide system but low Schmid factors for basal <a> and prismatic <a>. This is due to the strong texture which means a majority of grains belong to one main orientation mode.

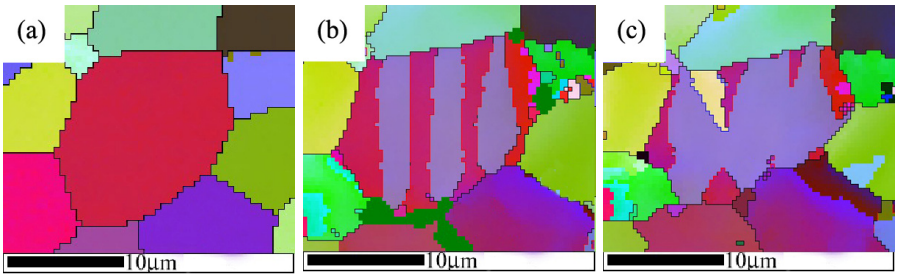

Figure 6: Initial grain with c axis close to the ND (dark red) (a); 10% deformation: $\{11\bar{2}2\}$ compression twins outlined by red lines (b); 20% deformation: a part of $\{11\bar{2}2\}$ twins undergoes secondary $\{10\bar{1}2\}$ tension twinning, (c). outlined by blue twinning boundaries delimiting the tension twin (in yellow colour).

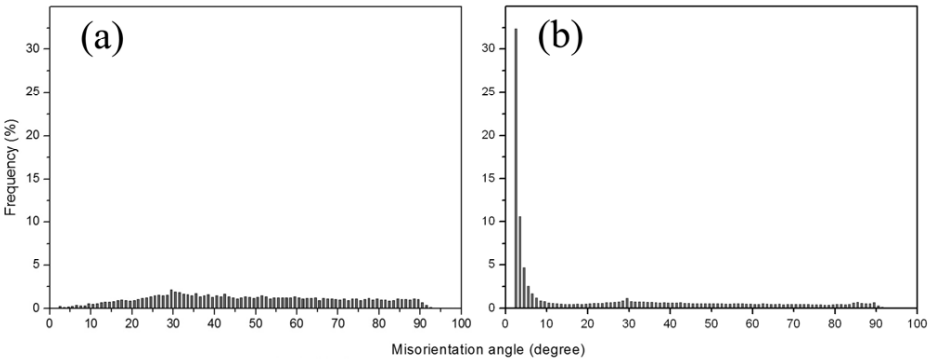

Figure 7: Misorientation-angle distribution, before compression (a) and after 20 % compression (b).

Table 2: Activated glide systems in 100 randomly selected grains.

Activated glide system	frequency
Basal <a>	11%
Prismatic <a>	51%
Pyramidal <a> or <c+a>	38%

5 Discussion

Orientation analysis indicates that at 10% reduction, the c-axis of the grains with $\{10\bar{1}2\}$ twins (tension along c-axis) is oriented close to the rolling direction, as shown in Fig. 8 (a), whereas that of the grains with $\{11\bar{2}2\}$ twins (compression along c-axis) is oriented close to the sample normal direction, as shown in Fig. 8 (b). These results are coherent with the theoretical expectations (Fig. 9). The c-axis of the $\{10\bar{1}2\}$ and $\{11\bar{2}1\}$ twinned part in each grain is systematically oriented close to a stable orientation belonging to the rolling texture component, however, the $\{11\bar{2}2\}$ twinning leads the c-axis of the twinned part oriented close to the rolling direction i.e. to an unstable orientation. As shown in Fig. 10, the $\{10\bar{1}2\}$ twinning reorientates the c-axis by 84.78°as schematized with the blue arrow in the figure. Likewise, the $\{11\bar{2}2\}$ twinning reorientates the c-axis by 64.62° as schematized with the red arrow. The green area is delimiting the stable orientation belonging to the rolling texture (characterized by c axes tilted about 30° from ND to TD). From the figure, we can see clearly that the $\{10\bar{1}2\}$ twinning reorientates the matrix to the stable orientation whereas $\{11\bar{2}2\}$ twinning acts reversely.

An interesting result of this study is that the effect of twinning on strain accommodation is to create a newly oriented zone (a new grain) and does not induce additional deformation mechanisms in the remaining matrix part of the grain. In other words, the deformation mechanisms in the matrix part of the twinned grains remain the same as those in the untwinned grains. The $\{11\bar{2}1\}$ and $\{10\bar{1}2\}$ twinning tend to reorientate the c-axes close to stable orientations. Thus, there is no tendency for secondary twinning to occur within such primary twins.

Secondary twinning only takes place in the $\{11\bar{2}2\}$ compression twins whose c-axes are orientated far away from the stable texture orientation. In such a case, the new and major twins appearing inside the $\{11\bar{2}2\}$ twins are $\{10\bar{1}2\}$ tension twins. This explains why when deformation is increased from 10% to 20% the amount of $\{10\bar{1}2\}$ tension twin dramatically increases. The c-axis of this secondary twin orientates towards the stable orientation. We could hardly observe the presence of any third-order twin, even after much higher deformation.

This can be easily understood by the relation between the geometrical and energet-

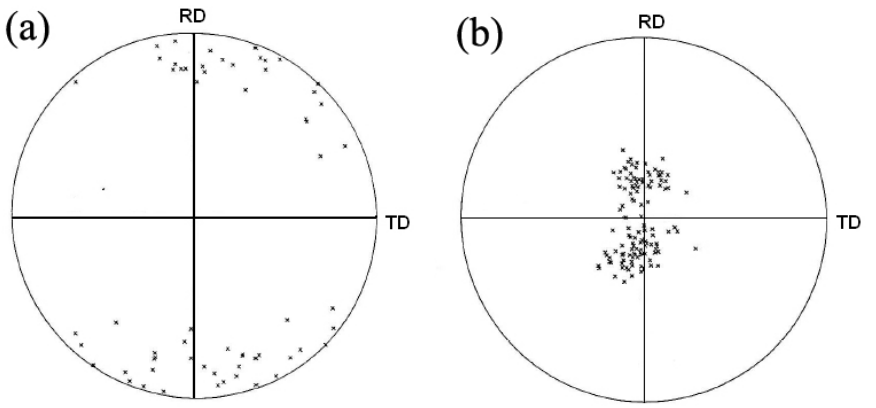

Figure 8: Initial {0002}-Pole figure of grains having $\{10\bar{1}2\}$ twin (a) and Initial {0002}-Pole Figure of grains having $\{11\bar{2}2\}$ twin (b) after 10% deformation.

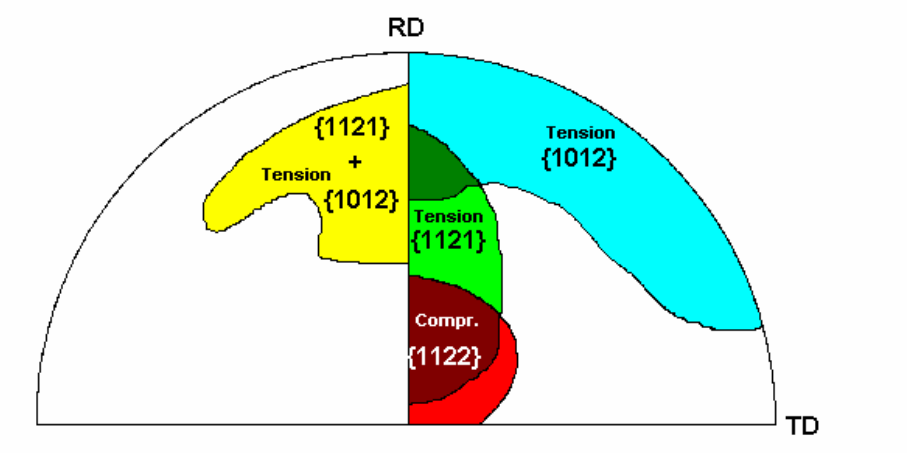

Figure 9: (0002) Pole Figure delimitating schematically the orientation domains of the c-axes of the grains in which the indicated twinning is expected to be activated (theoretical expectations).

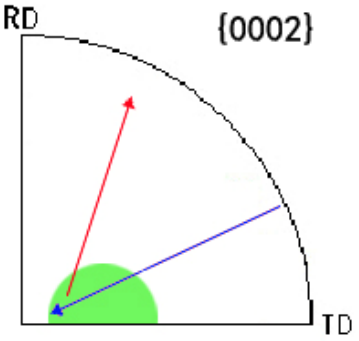

Figure 10: Schematical reorientation of c axes by $\{10\bar{1}2\}$ twinning (blue) and $\{11\bar{2}2\}$ twinning (red arrow).

ical characteristics of twinning. Several models have been developed to describe the nucleation of twin [Eshelby, J.D. (1957); Christian, J.W. (1958)]. These models are based on a "pole mechanism" i.e. a dislocation whose Burgers vector has a component normal to the twin planes equal to their spacing and a partial dislocation connected to this pole. The pole can be seen as a dislocation source and the partial dislocations are produced continuously in the planes parallel to the twin plane during deformation. If the path in which the partial dislocations move is short, the dislocations will easily be blocked, pile up and react to the source disabling it. Deformation twins always have a lenticular shape, since the interface can deviate from the twinning plane without greatly increasing the twin-interface energy [Partridge (1967)]. In addition, the strain energy increase should also be taken into account, approximately equal to $(c/r)\mu S^2$, where c and r represent the thickness and length of the twin, μ the shear modulus and S the twinning shear. Hence, secondary twins are already confined in a small volume due to the lenticular shape and cannot provide enough free path to develop a higher order twinning. In fact, in titanium alloys it is difficult to induce twinning at room temperature once the size of the matrix drops below the range of about 10 μm.

A major benefit of the interrupted "in situ" method is that we can follow the deformation process step by step. For example, in the grains having their initial c-axis close to ND for which secondary twinning occurs inside the primary twins, we can clearly discriminate the initial matrix from the primary twins thanks to the in-situ orientation information. In this case the primary twinned area is much larger than the remaining matrix and thus represents the "new matrix" for possible subsequent secondary twinning.

The effect of the neighboring grains slightly modifies the orientation in the vicinity of the grain boundary. This leads to a larger spread in the orientation measured in the vicinity of the grain boundary when the neighboring grain is strongly misoriented with respect to the considered grain.

Compared with rolling, channel die compression showed a simple deformation mode including only $\{10\bar{1}2\}$ tension twinning and various gliding. The primary reason is the simple stress condition applied in channel die compression. Therefore, we used the channel die compression results to clarify the effect of grain size on twinning.

357 grains with orientation favorable to the activation of $\{10\bar{1}2\}$ twinning were selected and divided into three groups according to their diameter. Group 1: 0 to 10 μm (221 grains); Group 2: 10 to 20 μm (129 grains); Group 3: 20 to 30 μm (7 grains). The calculated percentage of grains with twins for the three groups is shown in Fig.11. It is clear that with the similar orientation (c axis tilted $70^o \sim 90^o$ from normal direction ND), no twin occurs in the grains smaller than 10μm. With the increase of the grain size, the occurrence of the twin increases. Hence, grain size is an important factor affecting twin activation. The reason can be understood from geometrical and energetical considerations we introduced above.

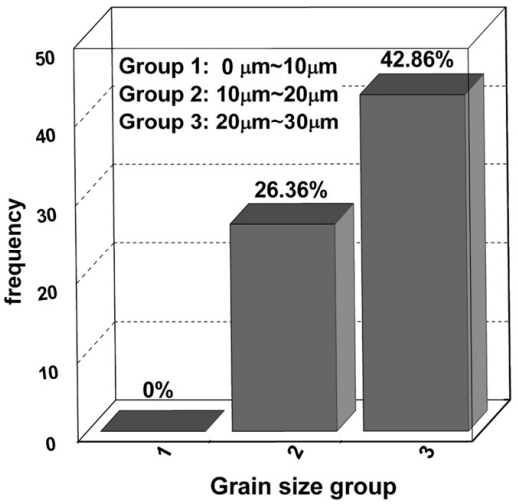

Figure 11: Percentage of twinned grains in the three different grain-size groups

6 Conclusion

Twinning occurs in grains having specific orientations. Generally, the reorientation induced by twinning aligns the c-axis of the twinned part to the stable rolling texture orientation, so that no further secondary twinning can be induced. Secondary twinning occurs only when the primary twinning orientates the c-axis of the primary twins far away from the stable orientations (this is generally the case for the $\{11\bar{2}2\}$ twinning). The formation of the $\{10\bar{1}2\}$ secondary twin inside the $\{11\bar{2}2\}$ primary twin results in a reorientation of the c-axis of the secondary twin to a stable orientation. Only a little amount of second order twin could be observed and twinning of higher than second order was not found.

The rotation of the matrix-part of the grains having twins is similar to that of the non-twinned grains with similar orientation. The twinned part of a grain can be considered as a new grain. When twins grow within the grain, they can consume almost the whole matrix. Special attention should be paid when determining the twinned volume fraction. With the EBSD measurement, a strong increase of the twinned volume could be demonstrated. This contradicts the conventional judgement that the twinned part is always the smallest part in a twinned grain, as concluded by optical microscopy. Only step by step EBSD orientation mapping allows an unambiguous determination of the twinned volume fraction. The confirmation that the order of twinning never exceeds the second order is very useful for the modeling polycrystalline plasticity in metals, such that the order allowed for twins should be restricted to only the first and second order (also called double twins).

Prismatic glide is the predominant glide system (51%), basal and pyramidal glide take 11% and 38% respectively. The relatively higher amount of pyramidal glide can related to the initial transverse or T-texture.

Acknowledgement: This work is supported by the FRAE project OPTIMIST and the French CNRS (PICS No. 4164). The authors would like to express their thanks to Mr. Patrick Moll at Laboratoire de Physique et Mécanique des Matériaux (LPMM CNRS FRE 3236) for the assistance to the channel die compression. The first author, Lei Bao is grateful for a PhD grant from China Scholarship Council.

References

Akhtar, A. (1975): Basal slip and twinning in α-titanium single crystals *Metallurgical and Materials Transactions A*. Vol. 6 pp. 1105-1113.

Akhtar, A.; Teghtsoonian, E. (1975): Dislocation sub-structure in α-Ti single crystals. *Journal of Crystal Growth.* Vol. 28 pp. 227-230.

Bunge, H.J.; Esling, C. (1984): Texture development by plastic deformation. *Scripta Metallurgica*. Vol. 18 pp. 191-195.

Bunge, H.J.; Esling, C.; Muller, J. (1980): *Journal of Applied Crystallography.* Vol. 13 pp. 544-554

Christian, J.W. (1958): Accommodation strains in martensite formation, and the use of a dilatation parameter *Acta Metallurgica.*Vol. 6 pp. 377-379.

Clement, A.; Coulomb, P. (1979): Eulerian simulation of deformation textures. *Scripta Metallurgica*. Vol. 13 pp. 899-901.

Eshelby, J.D. (1957): The Determination of the Elastic Field of an Ellipsoidal Inclusion, and Related Problems. *Proceedings of the Royal Society of London. Series A*. Vol. 241 pp. 376-396.

Field, D.P.; True, B.W.; Lillo, T.M.; Flinn, J.E. (2004): Observation of twin boundary migration in copper during deformation Matls. *Materials Science and Engineering A*. Vol. 372 pp. 173-179.

Jiang, L.; Jonas, J.J. (2008): Effect of twinning on the flow behavior during strain path reversals in two Mg (+Al, Zn, Mn) alloys. *Scripta materialia.* Vol. 58 pp. 803-806.

Jiang, L.; Jonas, J.J.; Mishra, R.K.; Luo, A.A.; Sachdev, A.K.; Godet, S. (2007): Twinning and texture development in two Mg alloys subjected to loading along three different strain paths. *Acta Materialia.* Vol. 55 pp. 3899-3910.

Kalidindi, S.R. (1998): Incorporation of deformation twinning in crystal plasticity models. *Journal of the Mechanics and Physics of Solids*, Vol. 46 pp. 267-284.

Kalidindi, S.R.; Bhattacharyya, A.; Doherty, R.D. (2004): Detailed analyses of grain-scale plastic deformation in columnar polycrystalline aluminium using orientation image mapping and crystal plasticity models. *Proc. Royal Society of London Series A*, Vol. 460 pp. 1935-1956.

Knezevic, M.; Kalidindi, S. R.; Fullwood, D. (2008): international jornal of plasticity. Vol. 24 pp. 1264-1276.

McDarmaid, D.S.; Bowen, A.W.; Partridge, P.G. (1984): Tensile properties of strongly textured Ti-6Al-4V after superplastic deformation. *Materials Science and Engineering*. Vol. 64 pp. 105-111.

Merriman, C.C.; Field, D.P.; Trivedi, P. (2008): Orientation dependence of dislocation structure evolution during cold rolling of aluminum. *Materials Science and Engineering A*. Vol. 494 pp. 28-35.

Panchanadeeswaran, S.; Doherty, R.D.; Becker, R. (1996): Direct observation of orientation change by channel die compression of a polycrystalline aluminum - Use of a split sample. *Acta Materialia*. Vol. 44 pp. 1233-1262.

Partridge, P.G. (1967): The crystallography and deformation modes of hexagonal close-packed metals. *Metallurgical, Review*. Vol. 12 pp. 169-194.

Philippe, M.J.; Esling, C.; Hocheid, B. (1988): Role of twinning in texture development and in plastic deformation of hexagonal materials. *Textures and Microstructures*. Vol. 7 pp. 265-301.

Philippe, M.J.; Serghat, M.; Van Houtte, P.; Esling, C. (1995): Modelling of texture evolution for materials of hexagonal symmetry-II. Application to zirconium and titanium α or near α alloys. *Acta Metallurgica et Materialia*. Vol. 43 pp. 1619-1630.

Pochettino, A.A.; Gannio, N.; Edwards, CVial.; Penelle, R. (1992): Texture and pyramidal slip in Ti, Zr and their alloys. *Scripta Metallurgia et Materialia* Vol. 27 pp. 1859-1863.

Prasannavenkatesan, R.; Li, B.Q.; Field, D.P,; Weiland, H. (2005): A parallel macro/micro elastoplasticiy model for aluminum deformation and comparison with experiments, *Metall. Mater. Trans A*, Vol. 36 pp. 241-256.

Quey, R.; Piot, D.; Driver, J.H. (2010): Microtexture tracking in hot-deformed polycrystalline aluminium: Experimental results. *Acta Materialia* Vol. 58 pp.1629-1642.

Skrotzki, W.; Toth, L.S.; Kloden, B.; Brokmeier, H.G.; Arruffat-Massion, R. (2008): Texture after ECAP of a cube-oriented Ni single crystal *Acta Materialia*. Vol. 56 pp. 3439-3449.

Vedoya, P.; Pochettino, A.; Penelle, R. (1988): Plastic Anisotropy of Titanium, Zirconium and Zircaloy 4 Thin Sheets. *Textures and Microstructures.* Vol. 8 pp. 601-610.

Yoo, M.H. (1981); Slip, twinning, and fracture in hexagonal close-packed metals. *Metallurgical and Materials Transactions A*. Vol. 12 pp. 409-418.